# VIP-expressing Dendritic Cells Protect Against Spontaneous Autoimmune Peripheral Polyneuropathy

Mehmet E Yalvac[1,2], William David Arnold[3,4], Syed-Rehan A Hussain[2], Cilwyn Braganza[2], Kimberly M Shontz[2], Kelly Reed Clark[1,2], Christopher M Walker[1,5], Eroboghene E Ubogu[6], Jerry R Mendell[1,2,4] and Zarife Sahenk[1,2,4]

*[1]Department of Pediatrics, The Ohio State University, Columbus, Ohio, USA; [2]Center for Gene Therapy, Nationwide Children's Hospital, Columbus, Ohio, USA; [3]Department of Physical Medicine and Rehabilitation, The Ohio State University, Columbus, Ohio, USA; [4]Department of Neurology, The Ohio State University, Columbus, Ohio, USA; [5]Center for Vaccines and Immunity, Nationwide Children's Hospital, Columbus, Ohio, USA; [6]Department of Neurology, University of Alabama, Birmingham, Alabama, USA*

The spontaneous autoimmune peripheral polyneuropathy (SAPP) model in B7-2 knockout nonobese diabetic mice mimics a progressive and unremitting course of chronic inflammatory demyelinating polyradiculoneuropathy (CIDP). In this study, bone marrow–derived dendritic cells (DCs) were transduced to express vasoactive intestinal polypeptide (VIP) using a lentiviral vector (LV-VIP). These transduced DCs (LV-VIP-DCs) were then injected intravenously (i.v.) into 16-week-old (before disease onset) and 21-week-old (after disease onset) SAPP mice in order to prevent or attenuate the disease. Outcome measures included behavioral tests, clinical and histological scoring, electrophysiology, real-time PCR, flow cytometry analyses, and enzyme-linked immunosorbent assay. LV-VIP-DCs were recruited to the inflamed sciatic nerve and reduced the expression of inflammatory cytokines. A single injection of LV-VIP-DC delayed the onset of disease, stabilized, and attenuated clinical signs correlating with ameliorated behavioral functions, reduced nerve demyelination, and improved nerve conduction. This proof-of-principle study is an important step potentially leading to a clinical translational study using DCs expressing VIP in cases of CIDP refractory to standard immunosuppressive therapy.

*Received 15 January 2014; accepted 21 April 2014; advance online publication 27 May 2014. doi:10.1038/mt.2014.77*

## INTRODUCTION

Chronic inflammatory demyelinating polyradiculoneuropathy (CIDP) is an acquired immune-mediated disorder of the peripheral nerves, with prevalence as high as 9/100,000.[1] The clinical features include weakness, sensory loss, imbalance, and impaired ambulation, which may lead to substantial disability. Corticosteroids, plasma exchange, and intravenous immunoglobulin, as the mainstay of treatment for CIDP, have all proven beneficial in randomized controlled trials.[2–5] Although these treatments are likely to be similar in efficacy, they differ in terms of their cost, availability, and adverse effects. Relapsing and remitting and refractory forms of CIDP require immunomodulatory agents such as azathioprine, cyclosporine, cyclophosphamide, interferons (IFN), methotrexate, mycophenolate mofetil, and rituximab, but they all cause serious side effects and are only effective in some patients. Thus, there is a need for new therapies.

Novel therapeutic strategies for CIDP require pertinent animal models. Experimental autoimmune neuritis may promote immunopathogenic understanding of demyelination, but limitations include a monophasic course with varying incidence and severity. In contrast, the spontaneous autoimmune peripheral polyneuropathy (SAPP) model in the B7-2 knockout, nonobese diabetic mouse provides a far better model to CIDP, its human counterpart. SAPP mice do not show diabetes, and the earliest onset of neuropathy is around 20 weeks of age with 100% of females and 30% of males affected.[6] The SAPP model has been well characterized representing an IFN-γ, $CD4^+$ T cell–mediated disorder, with autoreactive T cells and autoantibodies directed against myelin protein zero (P0).[7] This disorder is also associated with a reduction in antigen-specific $CD4^+$, $Foxp3^+$ T regulatory cells (Tregs) and has significant peripheral nerve infiltration of immune cells including $CD11c^+$ dendritic cell (DC), $CD4^+$, and $CD8^+$ T lymphocytes.[6,8] Parallel abnormalities in CIDP patients include a correlation between the number of $CD11c^+$, $CD14^-$, and $CD16^-$ myeloid DC in cerebrospinal fluid and clinical disability.[9] Reports also indicate a pathogenic role for $CD4^+$, $CD8^+$ T cells and concomitant reduction in circulating $CD4^+$, $CD25^+$ Tregs in CIDP patients.[10–12]

A novel therapeutic approach to SAPP mice with the potential for clinical translation has evolved from multiple reports of the potent anti-inflammatory effects mediated by the vasoactive intestinal peptide (VIP) that inhibit both innate and adaptive immune responses.[13] VIP is a 28-amino acid neuropeptide initially discovered in the lung and intestine.[14] It belongs to the secretin family with homology to pituitary adenylyl cyclase–activating

*Correspondence: Jerry R Mendell, Center for Gene Therapy, Nationwide Children's Hospital, Columbus, Ohio, USA. E-mail: Jerry.Mendell@nationwidechildrens.org or Zarife Sahenk, Center for Gene Therapy, Nationwide Children's Hospital, Columbus, Ohio, USA. E-mail: Zarife.Sahenk@nationwidechildrens.org*

polypeptide.[15] VIP inhibits the release of proinflammatory mediators by macrophages, promotes Th2 versus Th1 responses, and induces the generation of Tregs, making it attractive as a clinical translational tool for inflammatory disease. Experimental models of rheumatoid arthritis,[16] Crohn's disease,[17] uveoretinitis,[18] and experimental autoimmune encephalomyelitis[19] support its clinical value. Moreover, inhaled VIP showed immunoregulatory effects in sarcoidosis patients by increasing the number of peripheral Tregs.[20] However, the short half-life of systemic VIP and the pleotropic effects on the cardiovascular and gastrointestinal organ systems[21] limit its application. DC-mediated delivery of VIP can be an alternative approach to circumvent these shortcomings. In the experimental autoimmune encephalomyelitis model of inflammatory CNS disease, DCs expressing VIP, transduced by lentiviral vectors (LV-VIP-DC) demonstrated a robust therapeutic effect with reduced progression and increased survival of this mouse model for multiple sclerosis.[21]

The present experimental paradigm was initiated to explore the advantages of the LV-VIP-DC system for clinical translation targeting a peripheral nervous system inflammatory disease simulating refractory CIDP. The hypothesis tested was that the known peripheral nerve inflammatory infiltrates in the SAPP mouse would attract LV-VIP-DCs. Secretion of VIP in the nerve would suppress the $CD4^+$, $CD8^+$ T cell inflammatory infiltrate, induce tolerogenic DC (tDCs), and generate P0 antigen (Ag)-specific Tregs. The migration of tDCs with endocytosed degradative myelin products to regional lymphatic tissue would induce additional Ag-specific Tregs augmenting an anti-inflammatory/immunosuppressive effect. The net effect would enhance efficacy for patients with refractory and/or relapsing CIDP. For translation to a clinical setting, demonstrating efficacy in the SAPP mouse, a naturally occurring model of CIDP, provides clear advantages over an experimentally induced inflammatory nerve disease such as experimental autoimmune neuritis.

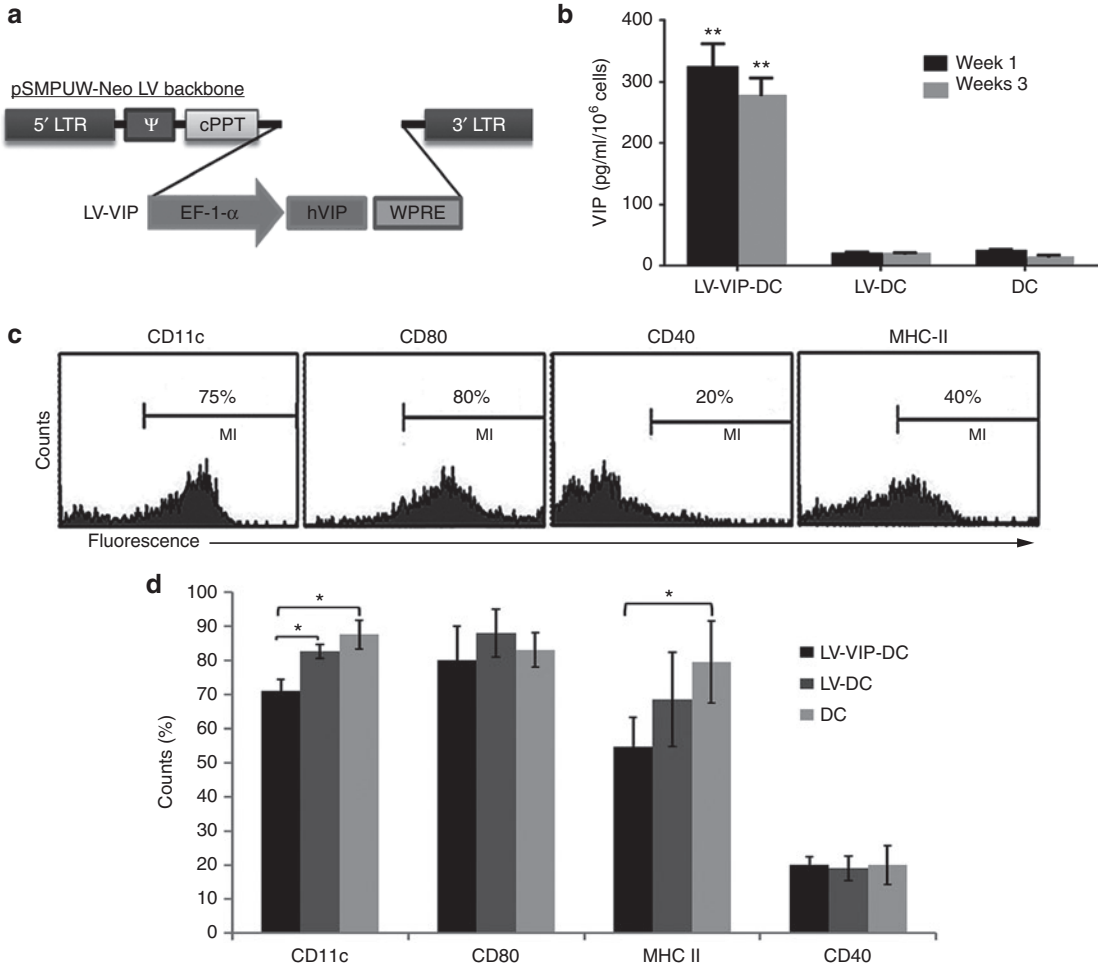


**Figure 1 Generation and characterization of LV-VIP-DC.** (**a**) Schematic representation of the LV cassette carrying VIP gene (LV-VIP). EF-1α promoter drives expression of hVIP cDNA in pSMPUW-Neo LV plasmid. (**b**) VIP secretion by LV-VIP–transduced dendritic cells (LV-VIP-DCs). LV-VIP-DCs and controls were cultured at a concentration of $1 \times 10^6$ cells/well for 24 hours, and the culture supernatant was analyzed for VIP levels using enzyme-immunoassay method. Error bars represent standard error of the mean (SEM) of four experiments. LV-DC, DCs transduced LV without hVIP cDNA. (**c**) Flow cytometry showing LV-VIP-DCs–expressing phenotypic markers, CD11c, CD80, CD40, and MHC-II at 3–4-day post-transduction. (**d**) Quantification of phenotypic markers, LV-VIP-DCs versus controls. Error bars represent SEM of five experiments. Statistical significance: $*P < 0.05$, $**P < 0.01$; one-way analysis of variance followed by Tukey's multiple comparison test. cPPT, central polypurine tract; DC, dendentric cell; EF, elongation factor; hVIP, human vasoactive intestinal polypeptide; LTR, long terminal repeat; LV, lentiviral vector; VIP, vasoactive intestinal polypeptide; WPRE, woodchuck hepatitis post-transcriptional regulatory element; ψ, cis acting elements.

## RESULTS

### Generation, characterization, and *in vivo* tracking of LV-VIP-DCs

Isolated DCs from the bone marrow of 4–6-week-old male SAPP mice were expanded for 3 days in the presence of recombinant murine granulocyte macrophage colony-stimulating factor (rmGM-CSF). On day 3, nonadherent cells were collected and transduced with third-generation LV–carrying human VIP gene (LV-VIP) under the control of elongation factor 1α promoter, known to sustain long-term gene expression in myeloid cells,[22,23] with a multiplicity of infection of 20 (**Figure 1a**). LV-VIP-DCs had an average of 0.7 ± 0.2 vector copy per cell and LV-DCs (DCs transduced with LV alone) had 0.5 ± 0.1 vector copy per cell (the results were given as mean ± SD of three different transduction experiments). Parallel experiments using LV-enhanced green fluorescent protein (EGFP) vector at multiplicity of infection of 20 showed that 45–50% of the DCs were EGFP positive in all after all transductions (**Supplementary Figure S1**). LV-VIP-DCs showed a sustained secretion of VIP for 3 weeks detected by using enzyme immunoassay (**Figure 1b**). Phenotypic analysis of LV-VIP-DCs was performed 3–4 days after transduction by using flow cytometry (**Figure 1c**). LV-VIP-DCs expressed phenotypic markers including CD11c (75%), CD80 (80%), CD40 (20%), and MHC-II (40%). LV-VIP-DCs were found to express CD11c significantly lower than nontransduced DC and LV-DC control groups. MHC-II expression in LV-VIP-DCs was significantly lower than DCs but not LV-DC alone (**Figure 1d**). Low expression levels of CD11c and MHC-II are linked to a tDC phenotype.[21] On bacterial lipopolysaccharide (LPS) stimulation, LV-VIP-DCs expressed significantly lower amount of CD40 than controls, which was also reported to be a feature of tDCs (**Supplementary Figure S2a**). Meanwhile, MHC-II levels were not

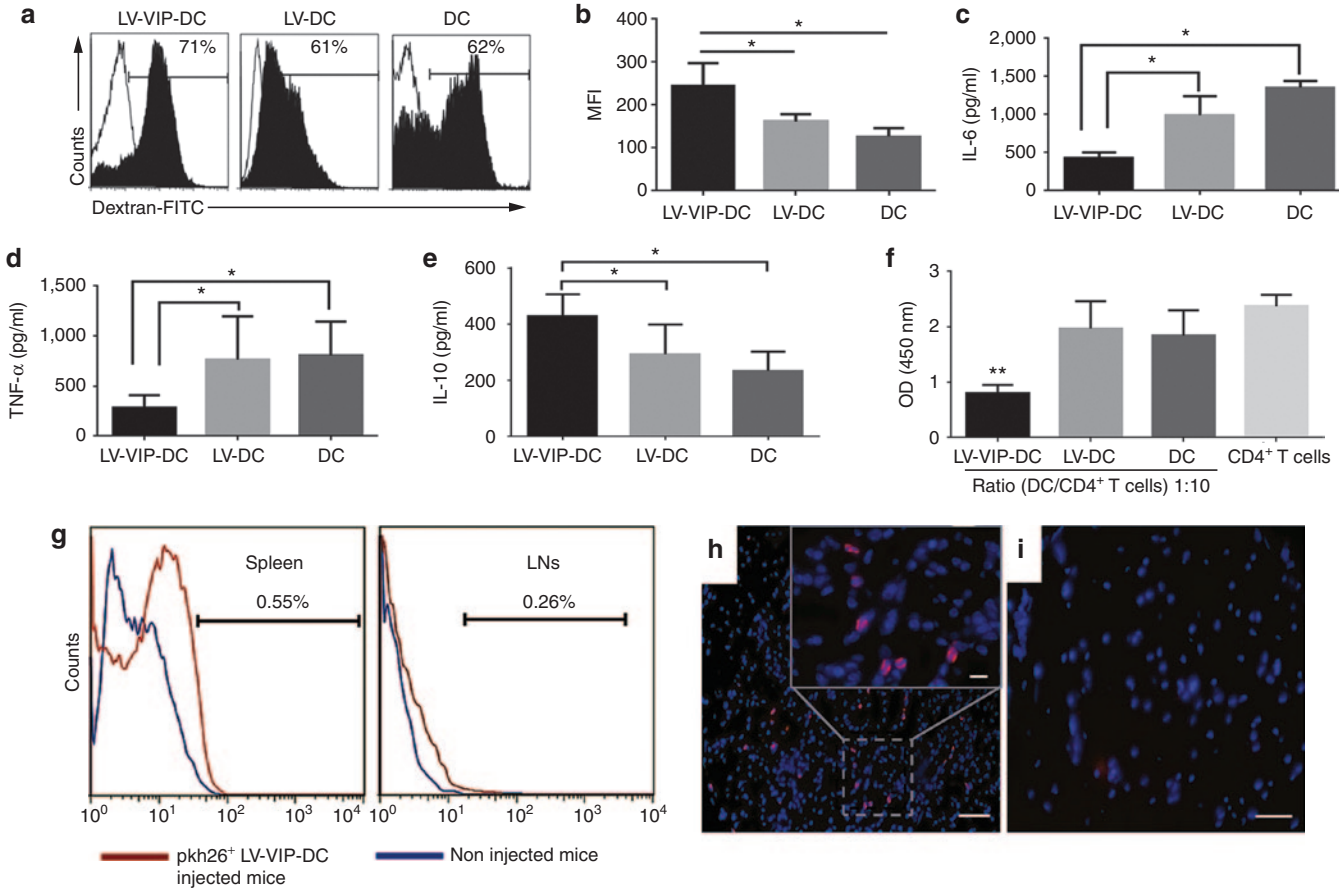


**Figure 2 Functional characteristics and *in vivo* tracking of LV-VIP-DCs.** (**a**) Endocytic capacity of LV-VIP-DCs and controls was determined 4–5 days after transduction by incubating the cells with 1 mg/ml dextran-FITC in medium for 3 hours at 4 °C (control; open histograms) or 37 °C (filled histograms) and analyzed by flow cytometry. (**b**) MFI were shown. LV-VIP-DCs were exposed to 1 µg/ml LPS in medium for 48 hours. The culture supernatant analysis shown at 24 hours for (**c**) IL-6, (**d**) TNF-α and at 48 hours for (**e**) IL-10. (**f**) LPS-induced LV-VIP-DCs, LV-DCs, and DCs were cocultured with splenic $CD4^+$ T cells ($2 \times 10^5$ cells/well) isolated from spontaneous autoimmune peripheral polyneuropathy (SAPP) mice in a 96-well plate in the presence of 5 µg/ml phytohemagglutinin and 50 U/ml IL-2 for 48 hours. Cell proliferation was determined by performing colorimetric BrdU cell proliferation assay. For **b–f**, the error bars represent standard error of the mean of three experiments done in triplicates; statistical significance: $^*P < 0.05$, $^{**}P < 0.01$; one-way analysis of variance followed by Tukey's multiple comparison test. (**g**) Pkh26-labeled LV-VIP-DCs ($3 \times 10^6$ cells) were injected into SAPP mice at 24 weeks of age ($n = 5$) and were detected in spleens and LNs at 48-hour postinjection by using flow cytometry. Sciatic nerves were removed 48-hour postinjection. Twelve-micrometer-thick cross-sections of sciatic nerve, which were viewed under fluorescent microscope, showed the presence of pkh26-labeled LV-VIP-DCs in the injected mice (**h**). (**i**) Sciatic nerve of noninjected mouse (scale bar = 50 µm; insert scale bar =10 µm). BrdU, 5-bromo-2′-deoxyuridine; DC, dendentric cell; FITC, fluorescein isothiocyanate; IL, interleukin; LNs, lymph nodes; LPS, lipopolysaccharide; LV, lentiviral vector; MFI, mean fluorescence intensities; pkh26, red fluorescent dye; VIP, vasoactive intestinal polypeptide.

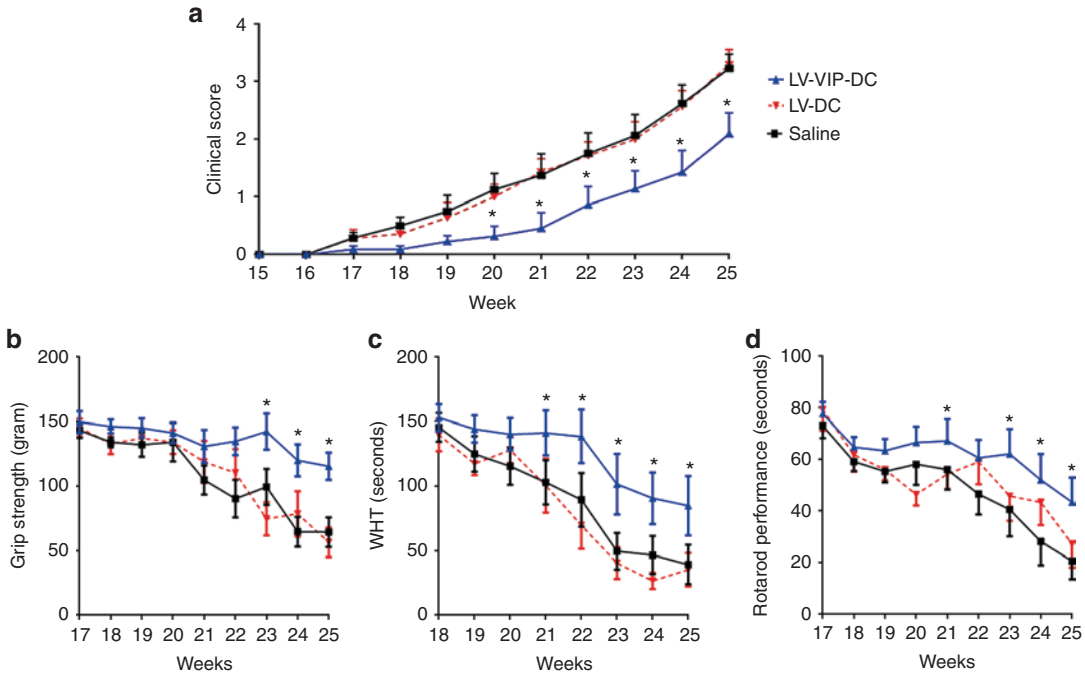


**Figure 3 LV-VIP-DC treatment delays the onset of disease and attenuates the disease progression.** (**a**) Clinical scores of spontaneous autoimmune peripheral polyneuropathy mice, injected with $3 \times 10^6$ LV-VIP-DC pulsed with P0 antigen at 16 weeks of age ($n = 11$) and control groups given either saline ($n = 11$) or $3 \times 10^6$ LV-DC ($n = 7$), followed weekly up to 25 weeks of age; see Material and Methods for clinical scoring. (**b**) Grip strength, (**c**) wire-hanging, and (**d**) rotarod tests were also performed weekly. Error bars represent standard error of the mean. Statistical significance between LV-VIP-DC and control groups was calculated by using two-way analysis of variance followed by Tukey's multiple comparison test; $^*P < 0.05$. DC, dendentric cell; LV, lentiviral vector; VIP, vasoactive intestinal polypeptide.

significantly different in all groups after LPS stimulation suggesting that LV-VIP-DCs have the same MHC-II-mediated antigen–presenting capacity as the LV-DCs and DCs have on maturation.

For further characterization of LV-VIP-DCs, their endocytic capacity was tested by incubating the cells with fluorescein isothiocyanate (FITC)-conjugated dextran for 3 hours followed by flow cytometry analysis. The results showed that LV-VIP-DCs had a higher endocytic capacity than DCs and LV-DCs (**Figure 2a**,**b**). The same trend was observed after the cells were exposed to LPS for 24 hours (**Supplementary Figure S2b**). To assess if the LV-VIP-DCs are functioning as tDCs, they were first exposed to LPS for 24 hours. On LPS treatment, LV-VIP-DC showed tDC-like functions by secreting significantly fewer proinflammatory molecules, interleukin (IL)-6, and tumor necrosis factor (TNF)-α compared to controls (**Figure 2c**,**d**). In addition, LPS stimulation gave rise to LV-VIP-DCs expressing higher amount of IL-10 than controls after 48-hour incubation (**Figure 2e**). When LPS-stimulated LV-VIP-DCs were cocultured with splenic $CD4^+$ T cells isolated from SAPP mice in the presence of phytohemagglutinin and IL-2, we found a significant reduction in T cell proliferation (**Figure 2f**). Taken together, these data provide evidence that *in vitro* generated LV-VIP-DCs demonstrate the characteristics of tDCs.

In another set of experiments for *in vivo* tracking of LV-VIP-DCs, we first injected $3 \times 10^6$ pkh26 (red fluorescent cell linker) labeled LV-VIP-DCs into SAPP mice i.v. At 48-hour postinjection, we detected the presence of pkh26-labeled LV-VIP-DCs in spleen and lymph nodes by analyzing the pooled cells using flow cytometry (**Figure 2g**). Moreover, histological examination of fresh-frozen sciatic nerve samples of injected mice revealed that pkh26-labeled LV-VIP-DCs were able to home to the sciatic nerve after i.v. injection (**Figure 2h**,**i**). DNA isolated from liver, lung, spleen, sciatic nerve, and lymph nodes of injected mice were analyzed to detect

**Table 1 Electrophysiological analysis of the sciatic nerve**

| Cohort | Group | *n* | Latency (ms) | Amp (mV) | CV (m/s) |
|---|---|---|---|---|---|
| Cohort 1 | | | | | |
| Baseline (16 weeks) | LV-VIP-DC | 11 | 0.8 ± 0.02 | 52.1 ± 3 | 64 ± 4.6 |
| | LV-DC | 7 | 0.7 ± 0.03 | 55.2 ± 3.1 | 61.6 ± 3.4 |
| | Saline | 11 | 0.8 ± 0.04 | 56 ± 2.6 | 56.8 ± 4.9 |
| End point (25 weeks) | LV-VIP-DC | 11 | 0.7 ± 0.2* | 35.5 ± 4.4** | 49.6 ± 5.2** |
| | LV-DC | 7 | 1.2 ± 0.5 | 7.4 ± 2 | 22.9 ± 2.2 |
| | Saline | 11 | 1.32 ± 0.6 | 11.8 ± 4 | 24.4 ± 5.2 |
| Cohort 2 | | | | | |
| Baseline (21 weeks) | LV-VIP-DC | 9 | 0.8 ± 0.03 | 49.5 ± 2.2 | 55.9 ± 3.4 |
| | LV-DC | 9 | 0.8 ± 0.02 | 52.4 ± 2.8 | 55.3 ± 3.6 |
| End point (25 weeks) | LV-VIP-DC | 9 | 0.8 ± 0.05* | 43 ± 4.8** | 50.16 ± 3.8** |
| | LV-DC | 9 | 1.2 ± 0.1 | 19.6 ± 3.6 | 24.8 ± 2.8 |

Data presented as mean ± SEM. Statistical significance between LV-VIP-DC and control groups (LV-DC and saline) at 25 weeks was calculated by using one-way analysis of variance followed by Tukey's multiple comparison test (cohort 1) and two-tailed *t*-test (cohort 2).
Amp, amplitude; CV, conduction velocity; DC, dendentric cell; LV, lentiviral vector; SEM, standard error of the mean; VIP, vasoactive intestinal polypeptide.
$^*P < 0.05$, $^{**}P < 0.01$.

the presence of LV-VIP-DCs by quantitative polymerase chain reaction (qPCR) using specific primers for woodchuck hepatitis post-transcriptional regulatory element region that integrates into LV-VIP-DCs genome after transduction. The results revealed that majority of the LV-VIP-DCs accumulated in the liver, lung, and spleen after 48-hour i.v. injection but only a small fraction of cells were detected in sciatic nerve and lymph nodes (**Supplementary Figure S3**). VIP serum levels of LV-VIP-DC-treated mice tested weekly up to 3 weeks using enzyme immunoassay test showed that LV-VIP-DC group had higher VIP levels at 1 week after treatment (**Supplementary Figure S4**).

## Therapeutic effect of LV-VIP-DCs in SAPP model

***Clinical observations and treatment cohorts in the SAPP mice.*** The natural history of neuromusclular weakness in saline-treated and LV-DC-treated SAPP is shown in **Figure 3a**. In this rederived SAPP colony at Nationwide Children's Hospital, clinical findings developed over a slightly accelerated time course compared to previously published results.[6,24] The onset of detectable mild tail weakness (mean clinical score of 0.5; see scoring system in Materials and Methods) occured at 17–18 weeks of age. A gradual mild to moderate weakness of fore or hind limbs ensued with clinical scores of 2 by 22–23 weeks, which rapidly became

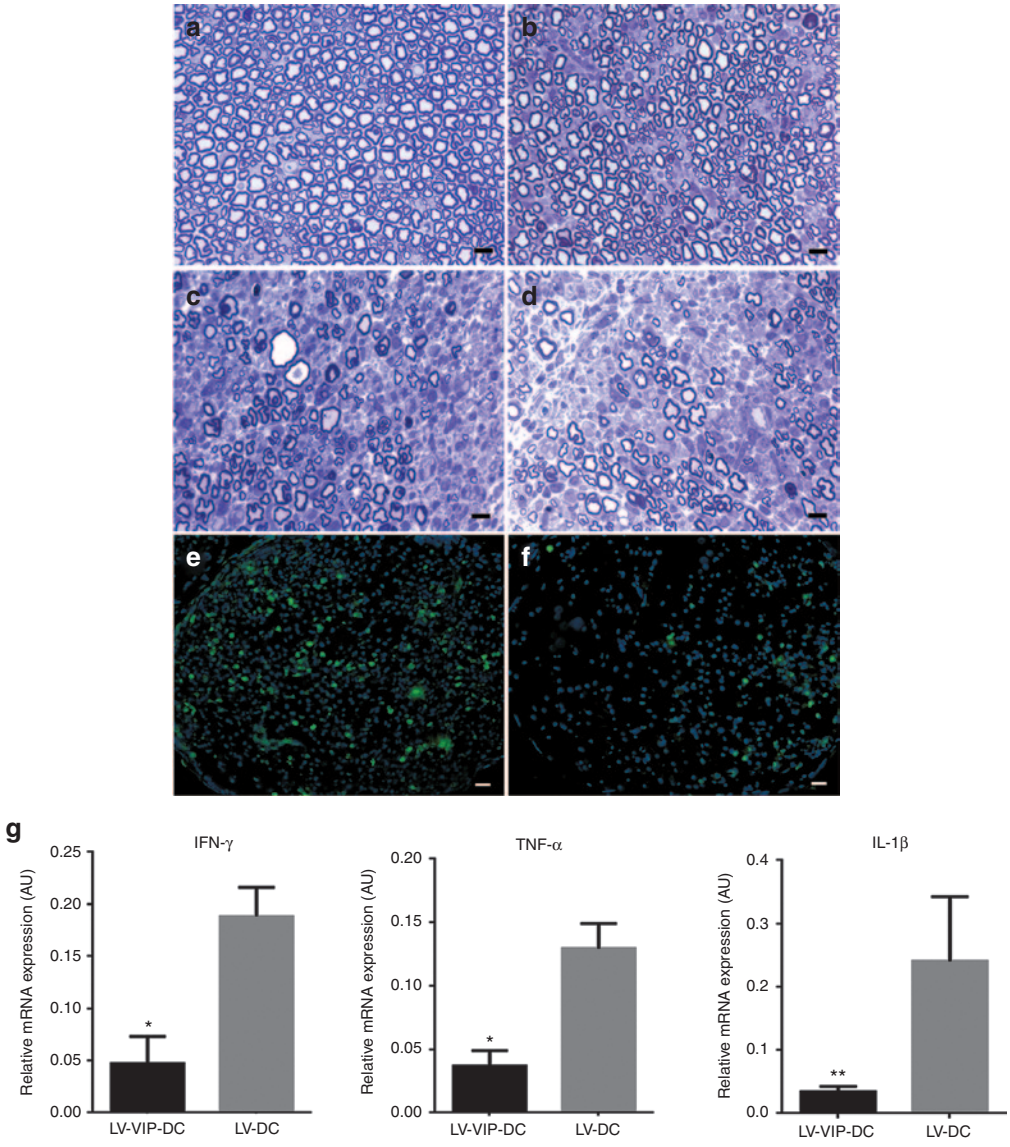


**Figure 4 LV-VIP-DC treatment protects myelinated fibers and reduces inflammation in sciatic nerve.** One-micrometer-thick cross-sections from midsciatic nerve segments before the disease onset at 16 weeks is shown in (**a**). Representative pictures of myelinated fibers from (**b**) LV-VIP-DC, (**c**) LV-DC, and (**d**) saline-injected groups at 25 weeks of age are shown. Scale bar = 10 µm. $CD3^+$ T cells infiltration in midsciatic nerve samples of (**e**) LV-DC and (**f**) LV-VIP-DC groups at 25 weeks of age. Scale bar = 10 µm. For quantitative data see **Table 2**. Expression levels of proinflammatory cytokines in sciatic nerves from LV-VIP-DC injected and LV-DC groups from cohort 1 at 25 weeks of age (**g**). Total RNA was extracted from snap frozen sciatic nerve samples and analyzed for expression of proinflammatory cytokines TNF-α, IL-1β, and IFN-γ by using real-time quantitative PCR. These data were normalized to glyceraldehyde 3-phosphate dehydrogenase. Error bars represent standard error of the mean ($n$ = 6–9 in each group; two-tailed $t$-test; $^*P < 0.05$, $^{**}P < 0.01$). AU, arbitrary units; DC, dendentric cell; IFN, interferon; IL, interleukin; LV, lentiviral vector; TNF, tumor necrosis factors; VIP, vasoactive intestinal polypeptide.

severe with mean scores of 3 by 25 weeks. Twenty-five weeks was selected as the end point for data collection because of observed rapidly evolving motor paralysis beyond that time point.

We tested the theraputic effect of LV-VIP-DC treatment in two cohorts of SAPP mice. Cohort 1 was treated at 16 weeks of age (before onset of symptoms) by i.v. delivery of $3 \times 10^6$ LV-VIP-DCs, pulsed with P0 (180–199) antigen for 16 hours. This experimental paradigm was designed to assess if nerve inflammation and demyelination can be prevented. A second group treated at 21 weeks of age assessed reversal or attenuation after clinical onset. Control groups were injected with saline or LV-DCs. The LV-DC controls avoided misinterpretation of an effect related to DC alone ensuring a distinction from a therapeutic effect related to LV-VIP-DCs. The mice were followed weekly, evaluating clinical scores and behavioral functions using grip strength, wire hanging, and rotarod tests. Treatment effect was also assessed by

**Table 2 Myelinated fiber density in the sciatic nerve**

| Cohort | Group | *n* | Myelinated fiber (number/mm²) | $CD3^+$ T cell (number/mm²) |
|---|---|---|---|---|
| Cohort 1 | LV-VIP-DC | 11 | 15,630.2 ± 2,100.8* | 307.3 ± 77.5** |
| | LV-DC | 7 | 8,114.8 ± 809.5 | 795.8 ± 92.2 |
| | Saline | 11 | 7,771.8 ± 1,596 | 780.1 ± 119.8 |
| Cohort 2 | LV-VIP-DC | 9 | 18,541.4 ± 2,368* | 361.8 ± 112.8* |
| | LV-DC | 9 | 8,937.7 ± 987.5 | 763.4 ± 91.9 |

Data presented as mean ± SEM. Statistical significance between LV-VIP-DC and control groups (LV-DC and saline) at 25 weeks was calculated by using one-way analysis of variance followed by Tukey's multiple comparison test (cohort 1) and two-tailed *t*-test (cohort 2).
Amp, amplitude; CV, conduction velocity; DC, dendentric cell; LV, lentiviral vector; SEM, standard error of the mean; VIP, vasoactive intestinal polypeptide.
*$P < 0.05$. **$P < 0.01$.

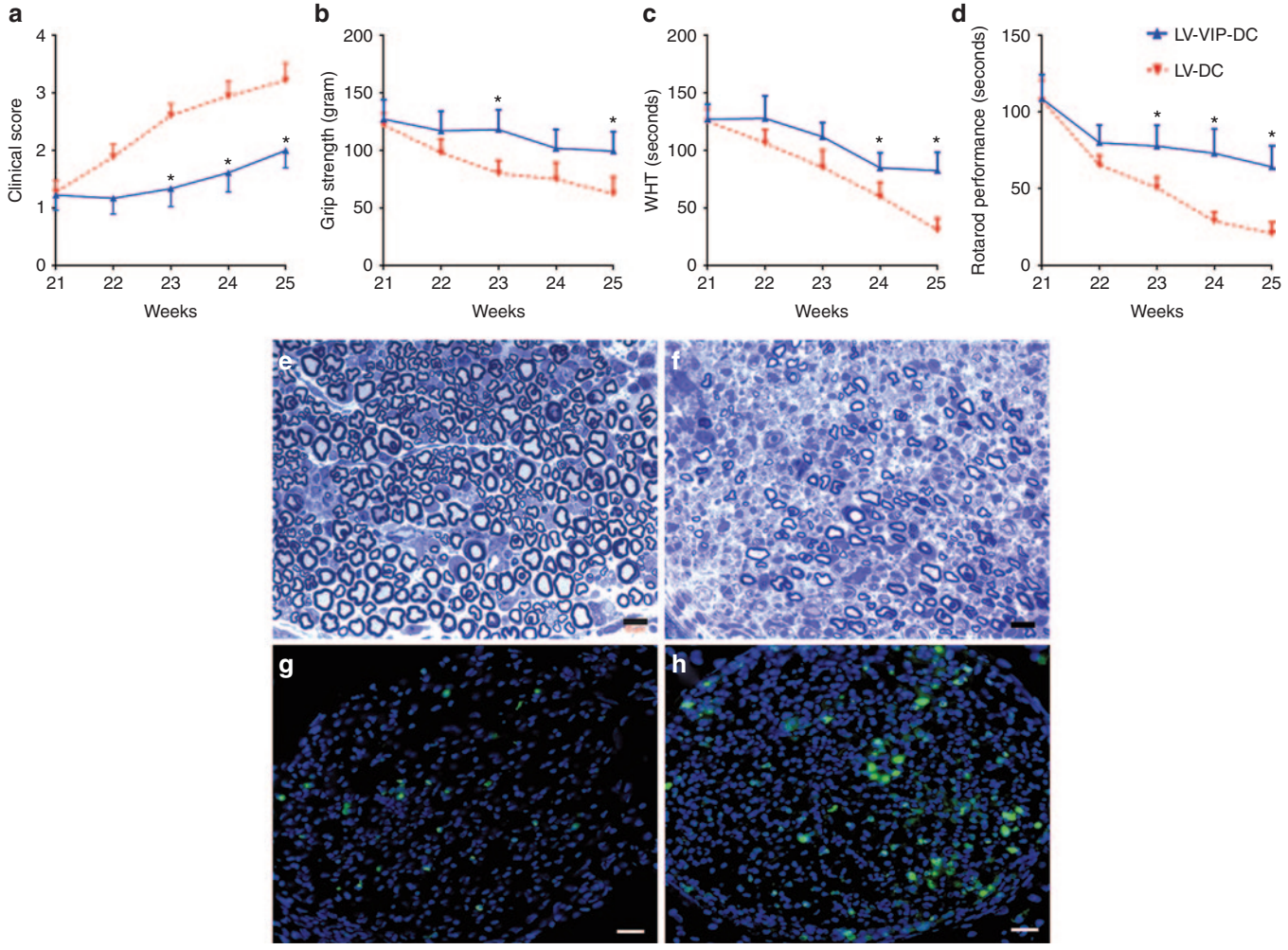


**Figure 5 LV-VIP-DCs stabilize and attenuate the disease progression.** Spontaneous autoimmune peripheral polyneuropathy mice were injected with $3 \times 10^6$ LV-VIP-DCs pulsed with P0 antigen at 21 weeks of age after disease onset. Control groups were injected with $3 \times 10^6$ LV-DCs. (**a**) Clinical scoring, (**b**) grip strength test, (**c**) wire-hanging test, and (**d**) rotarod test were performed weekly. Error bars represent standard error of the mean ($n = 9$ in each group). Statistical significance between LV-VIP-DC and control groups was calculated by using two-way analysis of variance followed by Bonferroni's multiple comparisons test (*$P < 0.05$). Representative 1-µm-thick cross-sections showing myelinated fibers from midsciatic nerves of (**e**) LV-VIP-DC and (**f**) LV-DC-injected control groups at 25 weeks. Bar = 10 µm. $CD3^+$ T cells infiltration in midsciatic nerve samples from (**g**) LV-VIP-DC and (**h**) LV-DC-injected mice at 25 weeks of age. Scale bar = 10 µm. DC, dendentric cell; LV, lentiviral vector; VIP, vasoactive intestinal polypeptide.

comparing baseline and end-point sciatic nerve conduction and histopathology studies.

***LV-VIP-DC treatment before the onset of clinical signs delays the onset of disease and attenuates the disease progression.*** The early signs of neuropathy were delayed to week 19–20 in the LV-VIP-DC-treated group (mean clinical score of 0.3 ± 0.2) at which time the disease was well established in control groups (mean clinical score of 1.1 ± 0.3 and 1 ± 0.2 in the saline- and LV-DC-treated groups, respectively) ($P < 0.05$). In addition, the treatment altered the progression of limb weakness, which was clearly attenuated reaching mild to moderate levels by 25 weeks in the LV-VIP-DC group (mean clinical score of 2 ± 0.3) compared to control groups showing severe hind limb weakness with the mean scores of 3.2 ± 0.3 in the saline and 3.3 ± 0.2 in the LV-DC groups ($P < 0.05$) (**Figure 3a**). Functional data in the SAPP mice following LV-VIP-DC treatment compared to control groups are shown in **Figure 3b–d**. Simultaneous bilateral hind limb grip strength, wire hanging, and rotarod performances showed gradual steady decline in the controls. In the LV-VIP-DC-treated mice, the rate of decline for these functions were clearly attenuated reaching a level of significance at 21 weeks of age for wire hanging test and rotarod ($P < 0.05$) and 23 weeks of age for hind limb grip strength ($P < 0.05$).

End-point sciatic nerve conduction studies at 25 weeks of age firmly established the efficacy of LV-VIP-DC treatment correlating with the clinical scores (**Table 1**, cohort 1). Compared to baseline, both saline- and LV-DC-injected groups showed statistically significant reductions in the mean compound muscle action potential (CMAP) amplitudes and conduction velocities with markedly prolonged distal latencies comparable to previously published findings in this model.[24] In the LV-VIP-DC-treated cohort 1, however, the percentage reductions in CMAP and conduction velocities from baseline were less pronounced indicating that this measure of disease progression was milder within the same period. In the LV-VIP-DC-treated SAPP mice, all three end-point sciatic nerve conduction parameters were significantly better than both control groups (**Table 1**, cohort 1). The CMAP amplitude, which provides a measure for the number of axons with preserved connections to muscle, was three to four times higher in the treated group compared to controls. Conduction velocity, a measure of saltatory conduction in the fastest conducting motor axons (a correlate of the degree of myelination in these axons), was two times faster in the treated group with significant shortening of the distal latencies.

Histological analysis of sciatic nerves correlated with clinical scores and electrophysiology. At 16 weeks of age, immediately prior to clinical onset of SAPP, 1-µm-thick cross-sections from midsciatic nerve segments showed normal appearing myelinated fiber population and myelinated fiber density (20,844.0 ± 319.8/mm$^2$; $n = 5$) (**Figure 4a**). LV-VIP-DC cell therapy had an unequivocal therapeutic effect (**Figure 4b**) compared to the control groups (**Figure 4c,d**). At week 25, the preservation of myelinated nerve fibers in the LV-VIP-DC-treated group was striking compared to the abundant changes in the controls including mononuclear leukocyte infiltration, endoneruial edema, demyelination, Wallerian degeneration, and a multifocal reduction in axonal density (**Figure 4c,d**). Thinly myelinated and solitary naked axons were encountered, as well as onion bulb formation associated with areas of persistent mononuclear cell infiltration compatible with an ongoing demyelinating/remyelinating neuritis model of CIDP.

The histological outcome of the treatment effect was quantifiably assessed by determining the myelinated fiber densities and inflammation at 25 weeks of age, permitting correlation with end-point electrophysiology. The results confirmed that LV-VIP-DCs treatment prevented significant myelinated fiber loss with

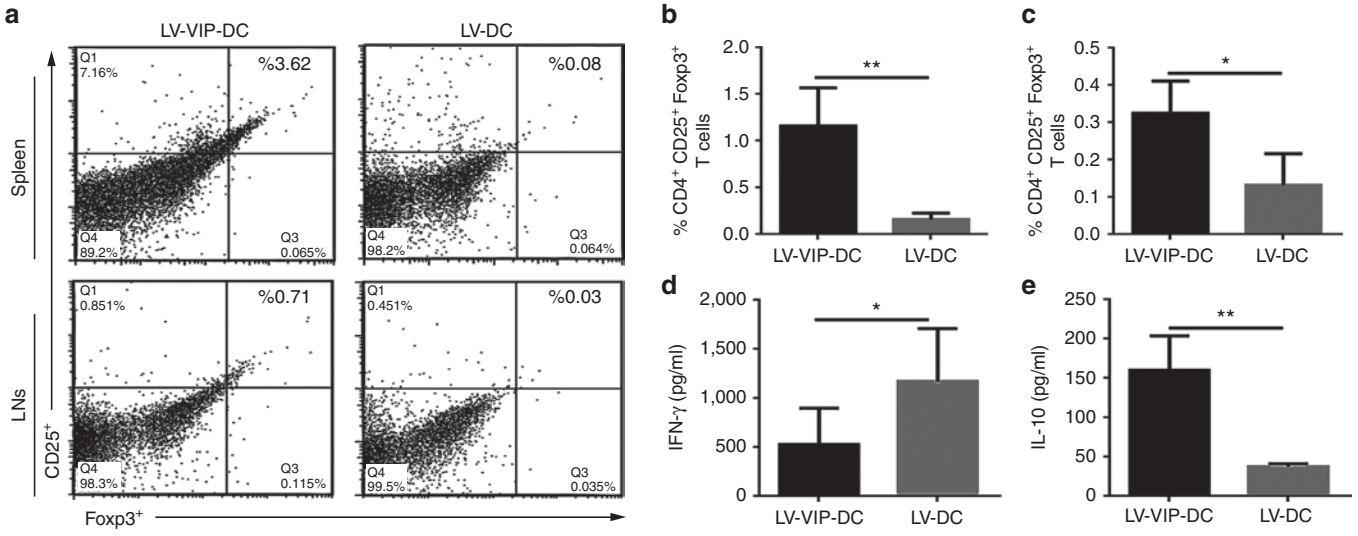


**Figure 6 Induction of Tregs and P0 antigen–specific responses.** At 25 weeks, splenocytes and LN cells were isolated and analyzed for Tregs. (**a**) A representative flow cytometry images of CD4$^+$, CD25$^+$, Foxp3$^+$ Tregs gated from CD4$^+$ T cells from spleen and LNs. Frequency of CD4$^+$, CD25$^+$, Foxp3$^+$ Tregs in (**b**) spleen and (**c**) LNs. Splenocytes were incubated in 12-well plate in the presence of 20 µg/ml P0 (180–199) in medium for 72 hours. (**d**) IFN-γ and (**e**) IL-10 levels in culture medium supernatant were detected by using enzyme-linked immunosorbent assay. Error bars represent standard error of the mean ($n = 7$–11 in each group). Statistical significance: two-tailed $t$-test (*$P < 0.05$, **$P < 0.01$). DC, dendentric cell; IFN, interferon; IL, interleukin; LN, lymph node; LV, lentiviral vector; Tregs, T regulatory cells; VIP, vasoactive intestinal polypeptide.

myelinated fiber density approximately two times higher in the LV-VIP-DC group (**Figure 4b**) than the controls (**Figure 4c,d**; **Table 2**, cohort 1). Compared to baseline values at 16 weeks, the mean myelinated fiber density at 25 weeks showed 25% reduction with treatment (20,844.0 ± 319.8/mm$^2$ versus 15,630.2 ± 2,100.8/mm$^2$) while a highly significant loss in the myelinated fiber population occurred in the LV-DC (20,844.0 ± 319.8/mm$^2$ versus 8,114.8 ± 809.5/mm$^2$) and saline-injected control (7,771.8 ± 1,596/mm$^2$) groups corresponding to 61 and 62.7% loss, respectively. In agreement with these findings, LV-VIP-DCs treatment decreased the CD3$^+$ cell content significantly compared to control groups injected with saline or LV-DC (**Figure 4e,f**; **Table 2**, cohort 1). Moreover, additional studies using real-time PCR to compare the expression of proinflammatory cytokines in sciatic nerves complemented these histopathological findings. LV-VIP-DC-treated group exhibited significantly reduced expression of IFN-γ, TNf-α, and IL-1β compared to the controls indicating reduced inflammation in the sciatic nerves (**Figure 4g**).

***LV-VIP-DCs given after disease onset stabilize and attenuate the disease progression.*** Cohort 2 SAPP mice received LV-VIP-DCs at 21 weeks of age to assess treatment reversal or attenuation at a later stage of disease. Baseline clinical scores were seen in treated (1.1 ± 0.2 in LV-VIP-DC) versus control groups (1.2 ± 0.3 in LV-DC control group; saline treatment omitted). In the LV-VIP-DC group, mean end-point clinical scores went up to 2 ± 0.3 while the control group showed significant worsening over the same period (mean score 3.2 ± 0.3) ($P < 0.05$) (**Figure 5a**). Functional data collected weekly in the cohort 2, SAPP mice are shown in **Figure 5b–d**. Similar to the LV-VIP-DC treated mice in cohort 1, we observed an attenuated rate of decline in the hind limb grip strength, wire hanging and rotarod performances by week 25 in each of these measures ($P < 0.05$). In agreement, sciatic nerve conduction parameters provided additional support for our conclusion that LV-VIP-DCs given after disease onset has a stabilizing and attenuating effect on the disease activity. In the LV-VIP-DC-treated SAPP mice, all three end-point sciatic nerve conduction parameters were significantly better than LV-DC injected controls (**Table 1**, cohort 2). Moreover, in the treated group, the percentage reductions in CMAP and conduction velocities from baseline were not significant while in the control group significant worsening was observed in these parameters. Compared to baseline, distal latency increased 33.3% (versus 2.5% in the treated) while the reduction in CMAP was 62.5% (versus 13.1% in the treated) and the slowing in conduction velocity was 55.1% (versus 10.3% in the treated) (**Table 1**, cohort 2). In accordance with these findings, the histological data revealed that LV-VIP-DC-treated group had twice the number of myelinated fibers and two times fewer CD3$^+$ T cells infiltrating the endoneurium compared to the LV-DC-treated group (**Figure 5e–h**; **Table 2**, cohort 2).

### P0 antigen–specific cytokine responses and induction of Tregs

In order to determine if LV-VIP-DC treatment resulted in an immunomodulatory response supportive of our hypothesis that VIP generated antigen-specific tolerogenicity, we analyzed splenocytes and lymph node cells for Tregs at week 25. We detected an increased percentage of CD4$^+$, CD25$^+$, Foxp3$^+$ Tregs in the spleen and lymph nodes in the LV-VIP-DC-treated SAPP mice (cohorts 1 and 2). A representative result from cohort 1 is shown in **Figure 6a–c**. In order to detect the antigen-specific responses, splenocytes were cultured for 72 hours in the presence of P0 (180–199), and the culture supernatant was analyzed for IFN-γ and IL-10 levels by using enzyme-linked immunosorbent assay. LV-DC-treated served as controls. IFN-γ levels were higher in LV-DC group indicative of a robust immune response against the P0 antigen (**Figure 6d**). Moreover, IL-10 levels in response to P0 (180–199) were higher in LV-VIP-DC-treated SAPP mice favoring induction of an antigen-specific tolerogenic response (**Figure 6e**). Ovalbumin (323–339), serving as control, produced no IFN-γ or IL-10 responses (data not shown). Overall, the findings indicate that LV-VIP-DC treatment generated antigen-specific immunomodulatory effects in favor of tolerogenicity.

## DISCUSSION

The findings of this study unequivocally demonstrate efficacy following a single injection of LV-VIP-DCs in SAPP mice, a spontaneously occurring autoimmune polyneuropathy mouse model for CIDP, its clinical counterpart. Both the mouse model and the clinical disease are characterized by an ongoing inflammation in the nerve, accompanied by demyelination/remyelination with secondary axonal loss. The SAPP model represents an IFN-γ, CD4$^+$ T cell–mediated disorder, with autoreactive T cells and autoantibodies directed against myelin protein P0.[6,7] There is a significant reduction in CD4$^+$, Foxp3$^+$ Tregs, and there are highly correlative immune abnormalities in the CIDP, the targeted clinical disease. The current study took advantage of previous reports of efficacy of VIP in animal models of rheumatoid arthritis,[16] multiple sclerosis,[25] and diabetes.[26] For most clinical autoimmune disorders, the potential therapeutic benefit of VIP is hampered by its short biological life and off-target effects. It is for this reason that we took advantage of DCs expressing VIP, transduced by lentivirus for the delivery of this potentially powerful anti-inflammatory agent. The results were unambiguous and set the stage for clinical translation.

Isolated bone-derived DCs transduced with VIP showed efficacy both in delaying the onset of inflammatory polyneuropathy and when further tested showed promise in the treatment of established neuropathy in SAPP mice. For this study, we started our own SAPP mouse colony that demonstrated an accelerated time course for the evolution of clinical signs of disease. Systemic i.v. delivery of LV-VIP-DCs to normal appearing SAPP mice at 16 weeks of age showed well-defined modulation of nerve inflammation, endoneurial edema, demyelination, and reduced inflammation at designed 25-week end point, after which mice are severely paralyzed. The LV-VIP-DC cohort was compared with saline-treated controls and with LV-DC controls. The latter done to avoid ambiguity potentially related to a DC effect. The efficacy findings were established in multiple domains including a clinical score, electrophysiological and histological analyses, and reduced inflammatory cell infiltration of the nerve. The clinical studies incorporated both an overall clinical score showing delayed onset and reduced disease progression. These studies were supported by improved performance of functional studies including hind limb grip strength, wire hanging, and rotarod performances. Nerve

conduction studies demonstrated less pronounced reduction of CMAP and conduction velocities compared to controls and histological studies correlated with clinical scores and electrophysiology. At 25 weeks, myelinated nerve fiber density was preserved, and findings such as endoneurial edema, mononuclear cell infiltration, demyelination, and Wallerian degeneration were markedly reduced.

We extended the study to address the treatment effect to a more clinically relevant phase of disease by administering LV-VIP-DCs after disease onset. Treatment was administered at week 21, and again, end-point parameters were improved in every outcome measure. The clinical scores were significantly improved compared to controls, again corroborated by individual nerve function. Sciatic nerve conduction studies showed better preservation of CMAPs (13.1% drop versus 62.5% controls), less reduction nerve conduction velocity (10.3% slowing versus 55.1% controls), and prevented prolongation of distal latencies (2.5% prolongation versus 33.3% controls). In the LV-VIP-DC-treated group, histological data revealed twice the number of myelinated fibers and far fewer $CD3^+$ T cells infiltrating the endoneurium.

The overall findings from this study support translation of this treatment approach to a clinical setting for CIDP patients not responding to standard methods of treatment. For these patients, the disease can be devastating. Our studies show an immunomodulatory effect mediated by VIP in support of our hypothesis. In addition to the direct benefits on nerve assessments, we detected an increase in $CD4^+$, $CD25^+$, $Foxp3^+$ Tregs in splenocytes and lymph node cells. Tregs are known to be diminished in CIDP,[12] and their overall increase in lymphatic tissue is another encouraging feature. Comparable measures of Tregs were difficult in mouse sciatic nerve requiring pooled sampling, and data from our study were not available. However, we were able to clearly demonstrate nerve-specific antigen tolerance in LV-VIP-DC-treated SAPP mice by showing an increase in IL-10 levels in response to P0 (180–199). As we continue to move these experiments toward a translational goal, we anticipate that further support for a clinically applicable protocol will come from a repeated LV-VIP-DC infusion paradigm that can be adopted to patients after disease onset. In addition, further studies showing a comparable effect using nonintegrating lentiviral vectors will be of value for clinical trials.

## MATERIALS AND METHODS

***Animals.*** SAPP breeding pairs were obtained from the Baylor College of Medicine and rederived in our transgenic core facility to avoid entry of a detected pathogen (fur mites) on mice into the facility. The study protocol was approved by The Research Institute at Nationwide Children's Hospital Animal Care and Use Committee and The Institutional Biosafety and Chemical Safety Committee.

***Reagents.*** Monoclonal anti-CD11c-FITC, CD80-PE, CD40-PE, MHC-II-PE, CD3-FITC, CD4-PE, and CD25-APC antibodies were purchased from BD Pharmingen (San Diago, CA). Anti-Foxp3-FITC, capture and biotinylated anti-mouse IL-10, TNF-α, IL-6 antibodies were purchased from eBioscience (San Diego, CA). rGM-CSF was purchased from Biolgend (San Diego, CA). All cell culture products were bought from Life Sciences (San Diego, CA) unless otherwise stated.

***Generation of lentiviral vectors.*** ViraSafe Lentiviral Expression System was purchased from Cell Biolabs (CA). hVIP cDNA was obtained from Origene (SC319768; OriGene Technologies, Rockville, MD). LV-VIP and LV-EGFP lentiviral vectors were designed by subcloning the hVIP cDNA and EGFP gene into the pSMPUW-Neo-LV expression plasmid backbone. Third-generation lentiviral vector particles were obtained by collecting 24- and 48-hour conditioned medium of 293 LTV cells, which were transfected with LV-VIP, LV-EGFP, or LV (backbone vector) vectors along with lentiviral packaging plasmids (Cell Biolabs). LV particles were concentrated by using ultracentrifugation and titrated using p24 ELISA Kit (Cell Biolabs) and by qPCR using qPCR Lentivirus Titration Kit (Applied Biological Materials, Richmond, ON, Canada). Aliquoted viruses were kept at −80 °C until use. LV-EGFP–transduced cells were analyzed by using flow cytometry.

***Generation of LV-VIP–transduced DCs.*** DCs were isolated as previously described.[27] Bone marrow cells flushed from femur and tibiae of 4–6-week-old male SAPP mice and cultured in 150-mm petri dishes with RPMI medium containing 10% fetal bovine serum (FBS), glutamax, 20 ng/ml rmGM-CSF, and 50 μmol/l 2-ME (DC medium). On day 3, nonadherent cells were collected and transduced with LV-VIP viruses (multiplicity of infection of 20). Briefly, $6 \times 10^6$ DCs were put into one well of 48-well plate in 400-μl serum-free RPMI media with 16 μg/ml polybrene (Sigma, MO, USA). The viruses were added into the media and mixed with DCs by gently pipetting. After 3 hours of incubation at 37 °C in 5% $CO_2$ incubator, 600-μl DC medium was added on top of the cells. Total volume was divided into two wells in a six-well plate, and 2.5-ml DC medium with 8 μg/ml polybrene was added into each well, and the cells were further incubated for another 12–16 hours with the virus. The cell media was replaced with fresh DC medium, and the cells were incubated for another 4–5 days. Vector copy per cell was determined by qPCR after all transductions.

***Flow cytometry analysis.*** $2 \times 10^6$ LV-VIP-DCs were incubated with fluorochrome-conjugated antibodies against CD11c, CD40, CD80, and MHC-II in 100-μl PBS for 45 minutes. For Treg analysis, $5 \times 10^6$ cells from spleens and lymph nodes of each mouse were first fixed with 1% paraformaldehyde and 0.05% Tween-20 in PBS overnight at 4 °C and then incubated with fluorochrome-conjugated antibodies against CD4, CD25, and Foxp3 in 200-μl PBS for 45 minutes. After incubation, excess amount of antibodies were washed twice with 1-ml PBS followed by centrifugation and resuspending the cells in 200-μl PBS for analysis. All flow analyses were performed using FACS Calibur flow cytometer (BD Biosciences, Mountain View, CA). Pkh26-labeled LV-VIP-DCs cells were prepared according to the manufacturer's instructions. Briefly, $10 \times 10^6$ DCs were resuspended in 500-μl Diluent-C and mixed with 500-μl Diluent-C mixed with 3 μl of pkh26 fluorescent linker dye. The DCs were stained for 5 minutes, and the reaction was stopped by adding 1-ml FBS followed by washing twice with PBS. The presence of pkh26-labeled LV-VIP-DC in spleen and lymph nodes was confirmed by the analysis of single-cell suspensions from spleen and lymph nodes using flow cytometry. Flow data were computed by using either CellQuest program (BD Biosciences) or the Flow Jo software (Tree Star, Ashland, OR).

***Enzyme immunoassay and enzyme-linked immunosorbent assay.*** LV-VIP-DCs were cultured ($1 \times 10^6$ LV-VIP-DCs/well) in a 48-well plate for 24 hours with fresh media, and the supernatants were collected. Serum samples were obtained from retro-orbital bleeds of treated and nontreated mice. All supernatants and serum samples were kept frozen at −80 °C until use. VIP levels in the supernatants and serum were analyzed by using enzyme immunoassay kit from Peninsula Laboratories (Belmont, CA) following the manufacturer's protocol. For the coculture experiments, splenic $CD4^+$ T cells from SAPP mice (>16 week old female) were isolated by using $CD4^+$ T cell isolation kit from Miltenyi Biotec (Auburn, CA) and cultured in a 96-well plate at a concentration of $2 \times 10^5$ cells/well in the presence of 5 μg/ml phytohemagglutinin (Sigma) and 50 U/ml IL-2 (Sigma) for 48 hours. Eight-day-old LV-VIP-DCs, LV-DCs, and DCs were first exposed to LPS (1 μg/ml) for 24 hours followed by washing and counting; then, they were cocultured

with $CD4^+$ T cells in a 96-well plate (DCs/T cell ratio was 1/10). Cell proliferation of $CD4^+$ T cells were determined by using 5-bromo-2′-deoxyuridine cell proliferation assay (Millipore, Bedford, MA) following the kit's instructions. Cytokine productions by splenocytes and DC were analyzed by using specific capture and biotinylated detection antibodies from eBioscience and following the manufacturer's instructions. The antigen peptides P0 (180–199) and ovalbumin (323–339) were purchased from Genescript (Piscataway, NJ) with the sequences as published in the literature.[7]

***Treatment and monitoring.*** Animals were divided into two treatment cohorts. First cohort was injected with $3\times10^6$ P0 (180–199) antigen primed LV-VIP-DC in 200-µl saline at 16 weeks of age (before disease onset), and the second cohort at 21 weeks (at disease onset) and followed up to 25 weeks of age. In both the cohorts, control mice were injected with either $3\times10^6$ P0 (180–199) primed LV-DCs in 200-µl saline or with 200-µl saline only. Clinical scores of animals were evaluated based on the scale from 1 to 6 as follows: 0 = normal strength, 1 = mild tail weakness, 2 = mild/moderate fore or hind limb weakness, 3 = severe fore or hind limb weakness, 4 = mild/moderate fore and hind limb weakness, 5 = severe fore and hind limb weakness.[24] Intermediate scores were given for asymmetrical hind or forelimb weakness. Functional tests included bilateral hind limb grip strength test, four limb wire-hanging test, and rotarod test following previously described and established protocols in our center.[28–30] All tests were performed weekly.

***Quantitative real-time PCR analysis (qPCR).*** Total RNA was extracted from snap frozen sciatic nerve samples of treated and control mice, for the expression analysis of cytokines (IL-1β, TNF-α, and IFN-γ), by using Trizol (Life Sciences). cDNAs were synthesized using transcriptor high fidelity cDNA synthesis kit (Roche, Mannheim, Germany). All qPCR analysis was performed using iTaq Universal SYBR Green Supermix (Biorad, Hercules, CA) according to the manufacturer's instructions. Specific primer sequences for IFN-γ were forward: GAGGAACTGGCAAAAGGATGG and reverse: TGTTGCTGATGGCCTGATTG. Other primer sequences for cytokines and housekeeping gene glyceraldehyde 3-phosphate dehydrogenase were obtained from the literature.[21] Real-time PCR analyses were performed by using ABI 7500 real-time PCR system (Applied Biosystems, Foster City, CA), and these data were computed by using Data Assist Software (Life Sciences). Forty-eight hours after the injection of cells ($3\times10^6$ cells/mouse) into SAPP mice (24 weeks old), the presence of LV-VIP-DCs in different tissues were detected based on qPCR analysis of woodchuck hepatitis post-transcriptional regulatory element region integrated into LV-VIP-DC genome by using specific primers for woodchuck hepatitis post-transcriptional regulatory element from Global ultra-rapid lentiviral titer kit (SBI, Mountain View, CA). Genomic DNA was isolated from tissues using QiaAMP Blood Mini Kit (Qiagen GmbH, Germany).

***Tissue allocation and histological analysis.*** Both the sciatic nerves were removed; one side was snap frozen for qPCR analysis. The proximal half of the other side in its *in situ* length was fixed in 3% glutaraldehyde in 0.1 mol/l phosphate buffer and further processed for plastic embedding according to the established methods in our laboratory.[31] The distal half was fixed in 4% paraformaldehyde overnight, cryoprotected and frozen in isopentane, and cooled in liquid nitrogen. One-micrometer-thick cross-sections from the plastic-embedded midsciatic nerves were used to generate myelinated fiber densities. In five randomly selected and digitally stored images photographed at ×60 objective, the number of myelinated fibers was determined using Axiovision software v 4.8.2.0 (Carl Zeiss MicroImaging, Munich, Germany), expressed as number per square millimeter of endoneurial area. Demyelinated or remyelinated axons containing thin myelin and axons undergoing Wallerian degeneration were excluded. In 12-µm-thick cross-sections from frozen sciatic nerves, $CD3^+$ T cell infiltration was assessed with immunohistochemistry using standard protocols. At least four randomly selected frames photographed at ×40 objective were used for counting of $CD3^+$ cells, and these data were expressed as number per square millimeter.

***Nerve conduction studies.*** Sciatic motor nerve conduction studies were performed bilaterally on each SAPP mouse under isoflurane anesthesia using a portable electrodiagnostic system (Synergy N2 EMG and nerve conduction study machine; Natus, Middleton, WI).[32] Distance for electrode placement was measured using a compass with a needle edge and a millimeter-graduated tape measure. The sciatic motor nerve conduction responses were recorded using two fine ring electrodes (Alpine Biomed, Skovlunde, Denmark) used as the active (E1) and reference (E2) electrodes. The hair of the hind limbs was removed using hair removal cream to allow appropriate electrode contact. The active recording electrode was placed over the mid portion of the gastrocnemius muscle and the reference electrode over the tendon. Using an irrigating syringe (Covidien, Mansfield, MA), the ring electrodes were precisely coated with electrode gel (Spectra 360; Parker Laboratories, Fairfield, NJ) to reduced skin impedance. A pair of 28 gauge monopolar needle electromyography electrodes (Teca, Oxford Instruments Medical, New York, NY) was used to deliver supramaximal stimulus to the sciatic nerve at the distal thigh and sciatic notch. The parameters measured included CMAP amplitude, distal latency, and conduction velocity.

***Statistical analysis.*** GraphPad Prism software (La Jolla, CA) was used for all statistical analyses. Clinical scores and functional tests were analyzed using two-way analysis of variance with Bonferroni or Tukey *post hoc* tests. The other experiment results having more than two groups were analyzed with one-way analysis of variance with Tukey *post hoc* test. Statistical difference of two groups was calculated by using two-tailed *t*-test. A value of $P < 0.05$ was considered statistically significant.

## SUPPLEMENTARY MATERIAL

**Figure S1.** Transduction of DCs with LV-EGFP.
**Figure S2.** Analysis of LV-VIP-DCs after LPS induction.
**Figure S3.** Tracking LV-VIP-DCs *in vivo*.
**Figure S4.** VIP levels in serum of treated animals.

## ACKNOWLEDGMENTS

This study was supported by GBS-CIDP Foundation International, and M.E.Y. is a Paul D. Wellstone Muscular Dystrophy Cooperative Research Center postdoctoral fellow. The authors declare that there are no conflicts of interest.

## REFERENCES

1. Laughlin, RS, Dyck, PJ, Melton, LJ 3rd, Leibson, C, Ransom, J and Dyck, PJ (2009). Incidence and prevalence of CIDP and the association of diabetes mellitus. *Neurology* **73**: 39–45.
2. Mehndiratta, MM and Hughes, RA (2002). Corticosteroids for chronic inflammatory demyelinating polyradiculoneuropathy. *Cochrane Database Syst Rev* **8**: CD002062.
3. Mehndiratta, MM, Hughes, RA and Agarwal, P (2004). Plasma exchange for chronic inflammatory demyelinating polyradiculoneuropathy. *Cochrane Database Syst Rev* **9**: CD003906.
4. Mendell, JR, Barohn, RJ, Freimer, ML, Kissel, JT, King, W, Nagaraja, HN *et al.*; Working Group on Peripheral Neuropathy. (2001). Randomized controlled trial of IVIg in untreated chronic inflammatory demyelinating polyradiculoneuropathy. *Neurology* **56**: 445–449.
5. Eftimov, F, Winer, JB, Vermeulen, M, de Haan, R and van Schaik, IN (2009). Intravenous immunoglobulin for chronic inflammatory demyelinating polyradiculoneuropathy. *Cochrane Database Syst Rev* **1**: CD001797.
6. Salomon, B, Rhee, L, Bour-Jordan, H, Hsin, H, Montag, A, Soliven, B *et al.* (2001). Development of spontaneous autoimmune peripheral polyneuropathy in B7-2-deficient NOD mice. *J Exp Med* **194**: 677–684.
7. Kim, HJ, Jung, CG, Jensen, MA, Dukala, D and Soliven, B (2008). Targeting of myelin protein zero in a spontaneous autoimmune polyneuropathy. *J Immunol* **181**: 8753–8760.
8. Bour-Jordan, H, Thompson, HL and Bluestone, JA (2005). Distinct effector mechanisms in the development of autoimmune neuropathy versus diabetes in nonobese diabetic mice. *J Immunol* **175**: 5649–5655.
9. Press, R, Nennesmo, I, Kouwenhoven, M, Huang, YM, Link, H and Pashenkov, M (2005). Dendritic cells in the cerebrospinal fluid and peripheral nerves in Guillain-Barré syndrome and chronic inflammatory demyelinating polyradiculoneuropathy. *J Neuroimmunol* **159**: 165–176.

10. Van den Berg, LH, Mollee, I, Wokke, JH and Logtenberg, T (1995). Increased frequencies of HPRT mutant T lymphocytes in patients with Guillain-Barré syndrome and chronic inflammatory demyelinating polyneuropathy: further evidence for a role of T cells in the etiopathogenesis of peripheral demyelinating diseases. *J Neuroimmunol* **58**: 37–42.
11. Schneider-Hohendorf, T, Schwab, N, Uçeyler, N, Göbel, K, Sommer, C and Wiendl, H (2012). CD8+ T-cell immunity in chronic inflammatory demyelinating polyradiculoneuropathy. *Neurology* **78**: 402–408.
12. Chi, LJ, Wang, HB and Wang, WZ (2008). Impairment of circulating CD4+CD25+ regulatory T cells in patients with chronic inflammatory demyelinating polyradiculoneuropathy. *J Peripher Nerv Syst* **13**: 54–63.
13. Delgado, M, Pozo, D and Ganea, D (2004). The significance of vasoactive intestinal peptide in immunomodulation. *Pharmacol Rev* **56**: 249–290.
14. Said, SI and Mutt, V (1970). Polypeptide with broad biological activity: isolation from small intestine. *Science* **169**: 1217–1218.
15. Vaudry, D, Gonzalez, BJ, Basille, M, Yon, L, Fournier, A and Vaudry, H (2000). Pituitary adenylate cyclase-activating polypeptide and its receptors: from structure to functions. *Pharmacol Rev* **52**: 269–324.
16. Delgado, M, Abad, C, Martinez, C, Leceta, J and Gomariz, RP (2001). Vasoactive intestinal peptide prevents experimental arthritis by downregulating both autoimmune and inflammatory components of the disease. *Nat Med* **7**: 563–568.
17. Abad, C, Martinez, C, Juarranz, MG, Arranz, A, Leceta, J, Delgado, M *et al.* (2003). Therapeutic effects of vasoactive intestinal peptide in the trinitrobenzene sulfonic acid mice model of Crohn's disease. *Gastroenterology* **124**: 961–971.
18. Keino, H, Kezuka, T, Takeuchi, M, Yamakawa, N, Hattori, T and Usui, M (2004). Prevention of experimental autoimmune uveoretinitis by vasoactive intestinal peptide. *Arch Ophthalmol* **122**: 1179–1184.
19. Gonzalez-Rey, E, Fernandez-Martin, A, Chorny, A, Martin, J, Pozo, D, Ganea, D *et al.* (2006). Therapeutic effect of vasoactive intestinal peptide on experimental autoimmune encephalomyelitis: down-regulation of inflammatory and autoimmune responses. *Am J Pathol* **168**: 1179–1188.
20. Prasse, A, Zissel, G, Lützen, N, Schupp, J, Schmiedlin, R, Gonzalez-Rey, E *et al.* (2010). Inhaled vasoactive intestinal peptide exerts immunoregulatory effects in sarcoidosis. *Am J Respir Crit Care Med* **182**: 540–548.
21. Toscano, MG, Delgado, M, Kong, W, Martin, F, Skarica, M and Ganea, D (2010). Dendritic cells transduced with lentiviral vectors expressing VIP differentiate into VIP-secreting tolerogenic-like DCs. *Mol Ther* **18**: 1035–1045.
22. Varma, NR, Janic, B, Ali, MM, Iskander, A and Arbab, AS (2011). Lentiviral Based Gene Transduction and Promoter Studies in Human Hematopoietic Stem Cells (hHSCs). *J Stem Cells Regen Med* **7**: 41–53.
23. Ramezani, A, Hawley, TS and Hawley, RG (2000). Lentiviral vectors for enhanced gene expression in human hematopoietic cells. *Mol Ther* **2**: 458–469.
24. Ubogu, EE, Yosef, N, Xia, RH and Sheikh, KA (2012). Behavioral, electrophysiological, and histopathological characterization of a severe murine chronic demyelinating polyneuritis model. *J Peripher Nerv Syst* **17**: 53–61.
25. Chorny, A, Gonzalez-Rey, E, Fernandez-Martin, A, Pozo, D, Ganea, D and Delgado, M (2005). Vasoactive intestinal peptide induces regulatory dendritic cells with therapeutic effects on autoimmune disorders. *Proc Natl Acad Sci USA* **102**: 13562–13567.
26. Sanlioglu, AD, Karacay, B, Balci, MK, Griffith, TS and Sanlioglu, S (2012). Therapeutic potential of VIP vs PACAP in diabetes. *J Mol Endocrinol* **49**: R157–R167.
27. Jing, H, Vassiliou, E and Ganea, D (2003). Prostaglandin E2 inhibits production of the inflammatory chemokines CCL3 and CCL4 in dendritic cells. *J Leukoc Biol* **74**: 868–879.
28. Sahenk, Z, Galloway, G, Edwards, C, Malik, V, Kaspar, BK, Eagle, A *et al.* (2010). TrkB and TrkC agonist antibodies improve function, electrophysiologic and pathologic features in Trembler J mice. *Exp Neurol* **224**: 495–506.
29. Klein, SM, Vykoukal, J, Lechler, P, Zeitler, K, Gehmert, S, Schreml, S *et al.* (2012). Noninvasive *in vivo* assessment of muscle impairment in the mdx mouse model – a comparison of two common wire hanging methods with two different results. *J Neurosci Methods* **203**: 292–297.
30. Payne, ET, Yasuda, N, Bourgeois, JM, Devries, MC, Rodriguez, MC, Yousuf, J *et al.* (2006). Nutritional therapy improves function and complements corticosteroid intervention in mdx mice. *Muscle Nerve* **33**: 66–77.
31. Sahenk, Z and Mendell, JR (1979). Ultrastructural study of zinc pyridinethione-induced peripheral neuropathy. *J Neuropathol Exp Neurol* **38**: 532–550.
32. Xia, RH, Yosef, N and Ubogu, EE (2010). Dorsal caudal tail and sciatic motor nerve conduction studies in adult mice: technical aspects and normative data. *Muscle Nerve* **41**: 850–856.